Longmate et al., https://doi.org/10.1083/jcb.201510042

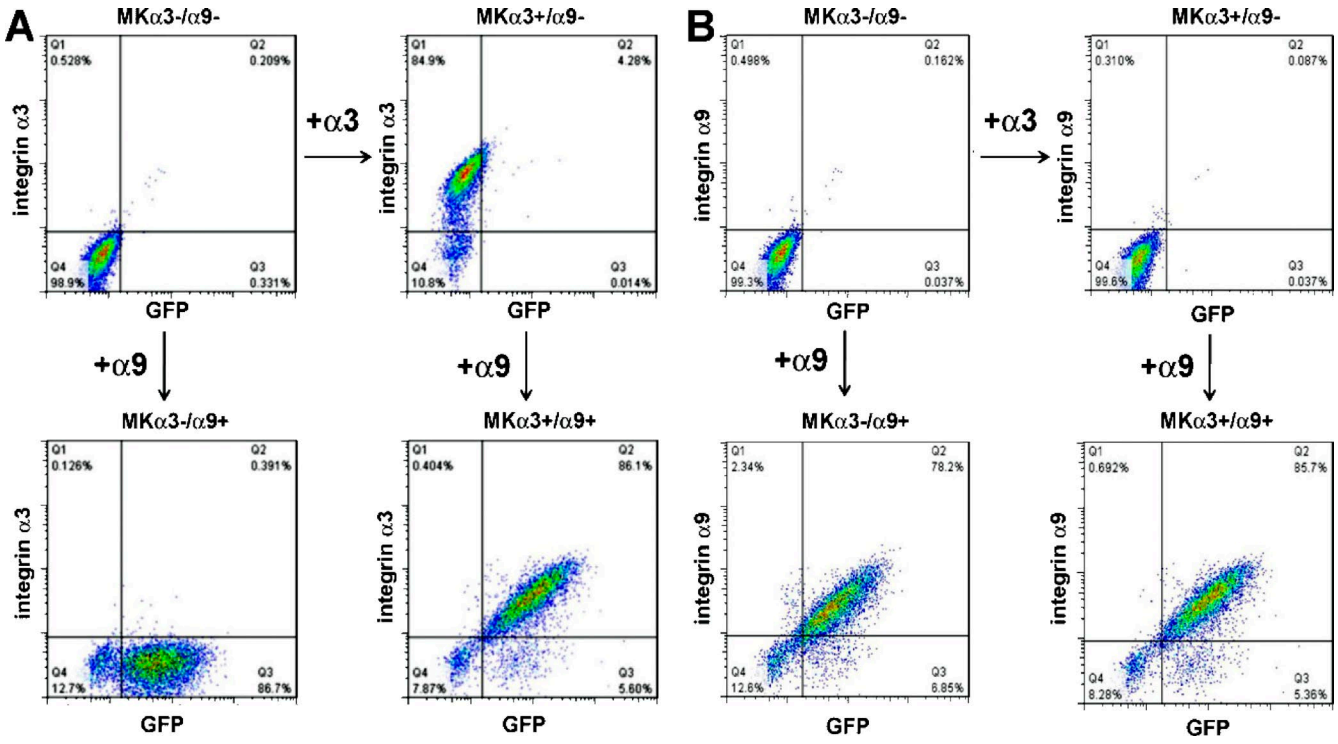

Figure S1. **Flow cytometry of integrins α3β1 and α9β1 on the cell surface of MK variants engineered to express the human α3 and/or α9 subunits in various combinations.** (A and B) MK genotypes are indicated over each plot. (A) Analysis of human α3 surface levels with mAb P1B5 (y axis) versus GFP (x axis) confirms appropriate expression of α3β1 and GFP (i.e., linked to α9 expression). (B) Direct analysis of human α9 surface levels with mAb Y9A2 (y axis) versus GFP (x axis) confirms linked expression of GFP and α9β1. "+α3" arrow indicates stable transfection with human α3; "+α9" arrow indicates stable transduction with retrovirally expressed human α9 linked to GFP expression through an IRES.

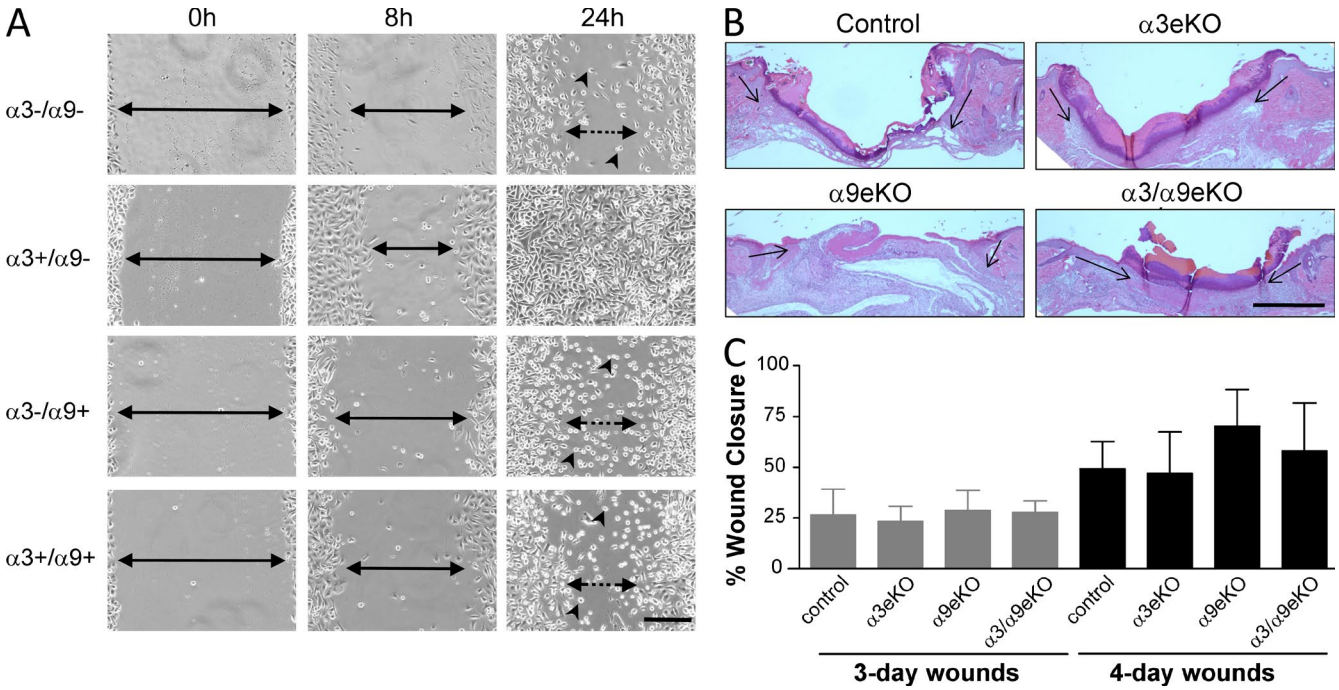

Figure S2. **α9β1 inhibits α3β1-dependent scratch wound closure in vitro but not wound reepithelialization in vivo.** (A) MK cell variants that express α3β1 and/or α9β1 in various combinations, as indicated, were grown to confluence on LN-332–rich ECM and then were subjected to scrape wounds. Wound edge morphology and migration were observed at 0, 8, or 24 h after wounding by phase microscopy. Results are representative of three independent experiments. Double-headed arrows indicate wound width, and arrows with dashed lines indicate poorly defined wound edges caused by cell scattering. Arrowheads point to examples of scattering cells. Bar, 100 µm. (B and C) In vivo wound reepithelialization was assessed by hematoxylin and eosin staining of 3-d and 4-d wounds from mice of each genotype. (B) Representative images of 3-d wounds are shown. Arrows indicate the length of the migrating wound epidermises originating from the wound edge. Bar, 500 µm. (C) Wound reepithelialization was quantified as follows: percent wound closure = ([length of epidermal tongue 1 + length of epidermal tongue 2]/length of wound bed) × 100. Means ± SEM are show. $n \geq 4$ mice per genotype.

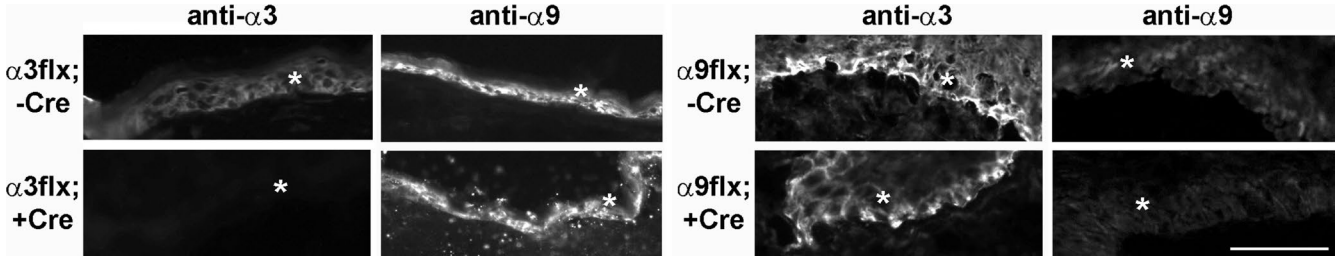

Figure S3. **Deletion of α3 or α9 integrin subunits in the epidermis of α3eKO or α9eKO mice, respectively.** Cryosections of 5-d fully reepithelialized wounds in mice homozygous for the floxed allele of either α3 or α9 and either lacking (–Cre) or expressing (+Cre) K14-Cre were immunostained with anti-α3 or anti-α9. Asterisks mark the epidermis. Bar, 50 µm.

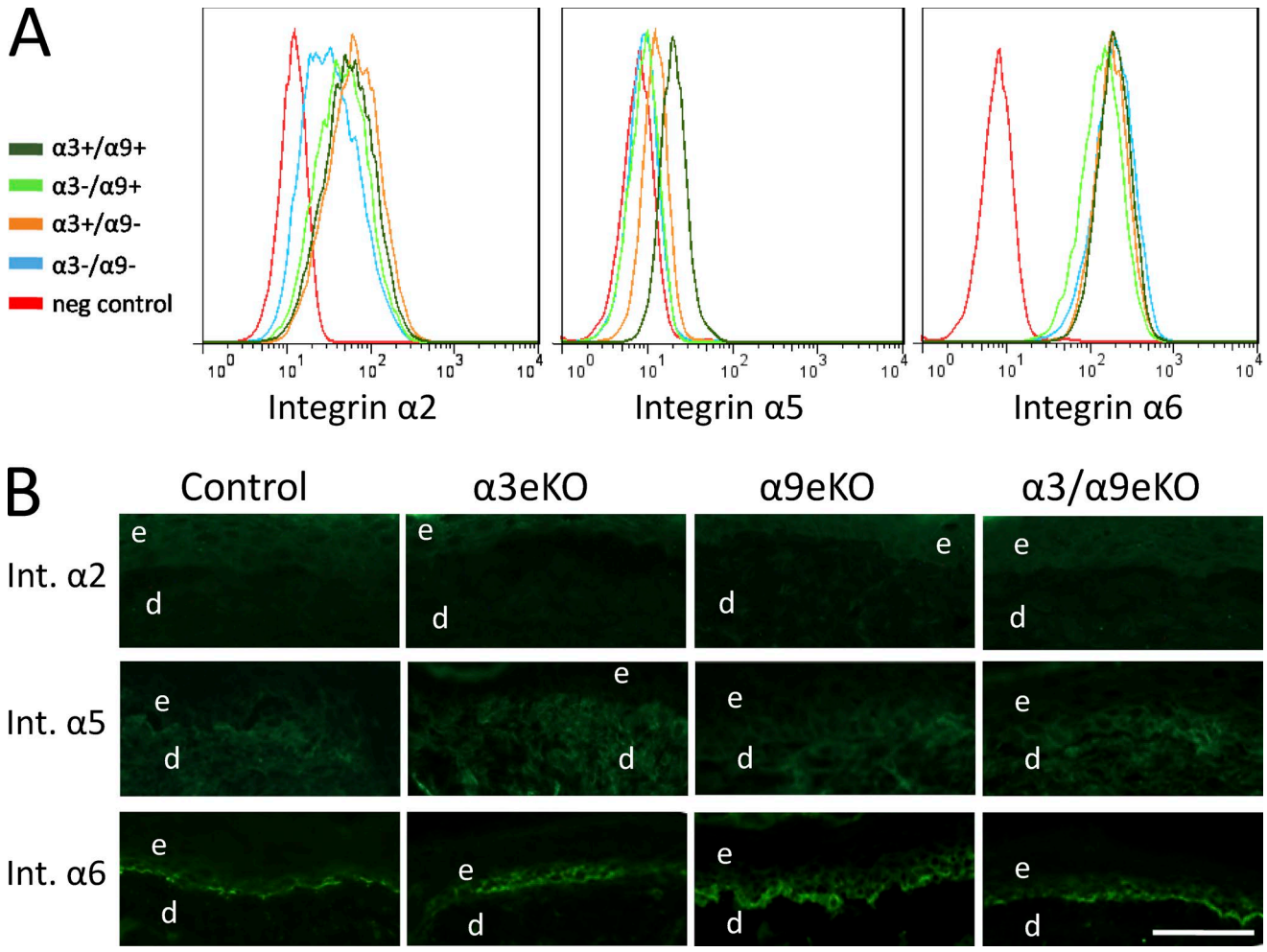

Figure S4. **Levels of other epidermal β1 integrins are not substantially altered in cells or mice with manipulated expression of α3β1, α9β1, or both.** (A) Flow analysis of mouse α2, α5 (both expressed at very low levels in resting skin), or α6 (expressed at high levels) confirms similar cell surface expression in MK variants. (B) Immunostaining for α2, α5, or α6 integrins performed on cryosections from the skin of control, α3eKO, α9eKO, and α3/α9eKO mice confirms similar expression in vivo. Bar, 100 μm. d, dermis; e, epidermis; Int, integrin; neg, negative.

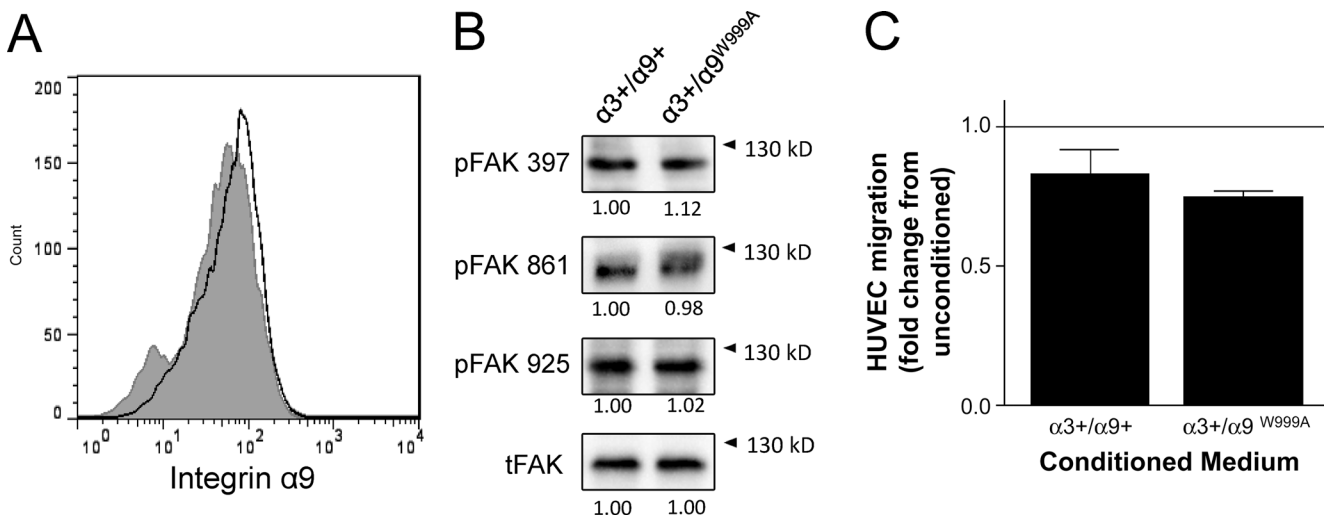

Figure S5. **The paxillin-binding site of the α9 subunit cytoplasmic tail is dispensable for suppression of the α3β1-dependent HUVEC migration response.** (A–C) MKα3$^+$/α9$^-$ cells were stably transduced with retrovirus encoding wild-type human α9 (see Fig. S1) or with a mutant of human α9 that cannot bind paxillin (α9^{W999A}; Liu et al., 2001; Young et al., 2001). (A) Flow cytometry demonstrates comparable surface levels of α9^{W999A} (black outline) and wild-type α9 (shaded area). (B) Cell lysates were assayed by immunoblotting for FAK phosphorylation at tyrosine residues Y397, Y861, or Y925, as indicated. Representative blots with positions of the 130-kD marker marked by arrowheads. Quantitations below each band represent the mean value from three independent experiments. The value for MK α3$^+$/α9$^+$ cells was set to 1.00 for each immunoblot. Note that exposure for each individual blot is optimized to compare signal intensity between wild-type α9 and α9^{W999A}, so phosphorylation differences between distinct tyrosines are not evident here as they are in Fig. 6. (C) Transwell assays were performed as in Fig. 1 to compare the HUVEC migration response to conditioned medium from MKα3$^+$/α9$^+$ or MKα3$^+$/α9^{W999A} cells. Graph shows HUVEC migration relative to that in cells treated with unconditioned medium as a baseline (set to 1.0). Means ± SEM are shown. *n* = 3 independent experiments. A Student's *t* test was used. P > 0.05.

References

Liu, S., M. Slepak, and M.H. Ginsberg. 2001. Binding of paxillin to the α_9 integrin cytoplasmic domain inhibits cell spreading. *J. Biol. Chem.* 276:37086–37092. http://dx.doi.org/10.1074/jbc.M105114200

Young, B.A., Y. Taooka, S. Liu, K.J. Askins, Y. Yokosaki, S.M. Thomas, and D. Sheppard. 2001. The cytoplasmic domain of the integrin α9 subunit requires the adaptor protein paxillin to inhibit cell spreading but promotes cell migration in a paxillin-independent manner. *Mol. Biol. Cell.* 12:3214–3225. http://dx.doi.org/10.1091/mbc.12.10.3214